Construction and Building Materials 250 (2020) 118928

Contents lists available at ScienceDirect

Construction and Building Materials

journal homepage: www.elsevier.com/locate/conbuildmat

The influence of nano-additives in strengthening mechanical performance of 3D printed multi-binder geopolymer composites

Mehdi Chougan [a,b], Seyed Hamidreza Ghaffar [a,*], Mohammad Jahanzat [a], Abdulrahman Albar [a], Nahzatullah Mujaddedi [a], Rafiq Swash [a]

[a] College of Engineering, Design and Physical Sciences, Brunel University London, Uxbridge, Middlesex UB8 3PH, United Kingdom
[b] University of Rome Tor Vergata, Department of Enterprise Engineering Mario Lucertini, Consortium INSTM RU Roma Tor Vergata, Via del Politecnico, 00133 Roma, Italy

HIGHLIGHTS

- Development of novel 3D printable geopolymer.
- Nano-additives improved the mechanical performance of 3D printed structures.
- The microstructural analysis revealed the micro-crack arresting effect of nano additives.
- The shape retention and buildability of geopolymer was improved with incorporation of nano additives.
- Rheology measurements play a crucial role in the selection of printable feedstock.

ARTICLE INFO

Article history:
Received 3 March 2020
Received in revised form 23 March 2020
Accepted 26 March 2020

Keywords:
Geopolymers
Nano-graphite platelets (NGPs)
3D printing

ABSTRACT

The weak mechanical properties the 3D printed parts can limit the competence of this technology when compared to conventionally cast-in-mold cementitious composites structures. However, experimental results in this study showed that the incorporation of nano additives could improve the mechanical property of printed structures. Six geopolymeric mixtures were designed and tested for their flow-ability, shape stability, buildability and mechanical performance. Different dosage of nano graphite platelets (NGPs) ranging from 0.1% to 1%, by the weight of geopolymer, were incorporated to the best performing geopolymer. The 3D printed geopolymer with 1% of NGPs increased the flexural strength by 89% and 46% compared to the same 3D printed and casted geopolymer without any NGPs, respectively. The same increase for compressive strength was 28% and 12%. Moreover, the geopolymer mix containing 1% of NGPs demonstrated the best shape retention and buildability.

1. Introduction

Additive manufacturing (AM) technology has the potential to transition the construction industry into a responsive and technically advanced sector, although, different grades of advanced printable feedstock needs to be formulated and developed to make this technology effective for the making of structural load bearing elements [1,2]. Strength reduction of 3D-printed parts due to the weak interlayer bonding is unavoidable and can impede the wider application of this eco-innovative manufacturing implementation in the construction industry [3–5]. Voids are formed when the printing of subsequent layers of materials are carried out, therefore, it leads to additional porosity during the manufacturing process. The formation of voids between layers reduce mechanical properties due to reduction in adhesion between printed layers. Zareiyan and Khoshnevis reported that the weak interlayer bonding could be attributed to (i) chemical forces in micro scale and (ii) interlocking and surface roughness in macro scale [4]. Moreover, one of the other challenges of 3D-printing implementation in the construction industry is the development of a printable raw material.

The negative environmental impact of ordinary Portland cement (OPC) has restricted the use of this material in advance construction methods such as 3D printing. However, many scientists shift to geopolymers as an eco-friendlier material. The term geopolymer is a typical name given to a new generation of covalently bonded synthesized amorphous materials containing chains of mineral molecule and/or 3-dimensional silico aluminate (Si-O-Al) structures [7–9]. Geopolymers have gained considerable

* Corresponding author.
E-mail address: Seyed.Ghaffar@brunel.ac.uk (S. Hamidreza Ghaffar).

https://doi.org/10.1016/j.conbuildmat.2020.118928
0950-0618/

interest due to their low setting time, high early-age strength gain, freeze–thaw resistivity, cost efficiency, and anti-corrosive properties [10–13]. However, the need for elevated temperatures to start geopolymerization as well as increasing the risk of eco-toxicity generated by the production of sodium silicate could potentially compromise the feasibility of these materials in large-scale constructions [14,15]. Several reinforcement methods (i.e. fibre reinforcement and nanoparticle reinforcements) have been reported to improve both interlayer bonding of 3D-printed geopolymer parts and low flexural strength of geopolymers [16,17]. Fibre reinforcement (i.e. polymer, glass, carbon, and steel fibres) could be one of the potential solutions to tackle the weak flexural strength of 3D-printed structures [17–20]. Hambach et al. (2017) also evaluated and compared the effectiveness of different fibre reinforcements (i.e. carbon, glass and basalt fibres) on the mechanical performance of OPC based 3D-printed parts [18]. The results revealed that the fibre alignment during the extrusion process exhibit a superior flexural strength up to 30 MPa. Bos et al. (2019) developed a short straight steel fibre reinforced printed mortar where the results showed that the steel fibres are able to improve the flexural strength of printed samples compared to casted specimens without steel fibres [19].

Only a few number of studies have been conducted which focus on the mechanical performance of 3D-printed geopolymers. Nematollahi et al. (2019) investigated the polypropylene fibre reinforced geopolymers in 3D-printing parts and improved the printing (i.e. shape retention and workability), and mechanical performance of geopolymers mortars all together [21].

Nanoparticle reinforcement of geopolymers can be considered as a novel development in the field of advanced construction materials. Amongst different proposed nano additives, carbon based materials (i.e. carbon nanotubes – CNTs, graphene nanoplates – GNPs, and graphene oxide – GO) have received more attention due to their high Young modulus, tensile strength and superior physical properties (i.e. electrical and thermal conductivity) [22,23]. Multi-walled Carbon Nanotubes (MWCNTs) were utilized in a number of investigations to modify the mechanical and physical properties of geopolymers, which led to a positive effect on geopolymers [24]. Saafi et al. (2013) added different dosages of MWCNTs in geopolymers, where an enhancement of 160%, 109% and 275% in flexural strength, Young modulus and flexural toughness was observed, respectively [25]. The same authors investigated the incorporation of other carbon-based materials in geopolymers. The results revealed that the addition of reduced graphene oxide (rGO), significantly refine the porous structure and increase the electrical conductivity of geopolymers. The results showed 134%, 376% and 56% increase in flexural strength, Young modulus, and flexural toughness, respectively [26]. Ranjbar et al. (2015) reported the effect of incorporation of GNPs on mechanical properties and morphology of geopolymers. The results revealed that the addition of 1% GNPs increased the flexural and compressive strength by 2.16 and 1.44 times compared to plain geopolymers, respectively [27].

Despite the noble improvement achieved by the addition of carbon-based materials in geopolymers, no research, to the best of authors' knowledge, has previously studied the effectiveness of graphene nanoparticles (NGPs) incorporation in geopolymers for 3D printing applications.

The incorporation of nano graphite in geopolymer offers several applications in the field of smart constructions, including underfloor heating, high-speed train lines, high-voltage transmission pipelines, and de-icing roads generated by the increase in thermal conductivity of cementitious composites [28,29]. Moreover, it can induce self-sensing properties due to the increase in electrical conductivity, which contributes to identifying and monitoring the defects initiations within the structure and reduces the maintenance costs [30]. The one factor, which can compromise the extensive use of these nanofillers, is their high costs. According to the supplier (Asbury Carbons, USA), the price for a laboratory-scale test is about $668.12 per 2.3 kg. The estimated cost for 1% nano graphite per 1 kg of geopolymer is about $1.24. Chougan et al. (2019) also reported that the production of graphene-based materials in the industrial-scale could drop the price down by about 70% [31].

In this study, a printable geopolymer was optimised and selected from several mix designs, based on fresh and hardened properties evaluated for both printed and traditionally casted samples. Subsequently, the two mix designs with adequate printing properties (i.e. fresh properties) and minimum mechanical performance gap between printed and casted specimens were identified. Further tests, i.e. rheology and buildability were executed to identify the best mix out of the two options. The best mix was reinforced by 0.1%, 0.3%, 0.5% and 1% of nano-graphite platelets (NGPs). Several tests (i.e. rheology, shape retention, shape stability, structural build-up, and microstructural analysis) were performed to characterize the reinforced geopolymer mix. The objective was to evaluate the overall performance of 3D printed NGP reinforced geopolymers in comparison to un-reinforced casted samples.

2. Experimental methodology

2.1. Materials

The raw materials used in this study consisted of: 1) Fly ash (FA) obtained from Cemex, (BS EN 450-1:2012). 2) Ground-granulated blast furnace slag (GGBS) obtained from Hanson UK. 3) Silica fume (SF) obtained from J. Stoddard & Sons Ltd. 4) 98% pure sodium hydroxide (NaOH) (Fisher Scientific, Germany). 5) Sodium silicate (Na2SiO3) (Solvay SA, Portugal). 6) Nano-graphite platelets (NGPs), 97.5% purity and lamella thickness index approximately 6–7 nm, obtained from Grade Nano99 by Asbury Carbons USA. A 10 M sodium hydroxide solution was prepared by dissolving sodium hydroxide pellets in de-ionized water and allowed to cool before use. Sodium silicate had a SiO2/Na2O: 3.23 (8.60 wt% Na2O, 27.79 wt% SiO2, 63.19 wt% H2O, 0.4 wt% Al2O3).

The micro-morphology of FA, GGBS, SF and NGP were observed using a scanning electron microscope (SEM) (Supra 35VP) as shown in Fig. 1. A Sequential benchtop Wavelength Dispersive X-ray Florescence (WD-XRF) spectrometer (Supermini200) mounted with LiF (2 0 0) and PET crystals was used to obtain the chemical composition of FA, GGBS and SF, of which the main oxides are presented in Table 1. The mineralogical compositions of Nano-graphite platelets (NGPs) was obtained by powder X-ray diffraction (XRD) (D8 Advance) diffractometer with an automatic slit, mono-chromated CuKα radiation (λ = 1.5405 Å), 5–70° 2θ range, with steps of 0.02°/2θ and 0.5 s/step. Peak shapes were studied using the program DIFFRACT.SUITE (Bruker, Germany) and the results are shown in Fig. 2. The XRD patterns of FA, GGBS and SF based on previous studies [32] revealed that, FA has partly amorphous behaviour (between 2θ 5° and 2θ 30°) along with small crystalline phases of Quartz, Mullite, anhydrite and magnetite. GGBS and SF behaved as amorphous without any significant crystalline phases. It is important to emphasise that the presence of such materials with amorphous structure helps the geopolymerization by dissolving more efficiently in alkaline activators [6]. For NGPs (see Fig. 2) the hexagonal graphite characteristic peaks (the main peak at 2θ: 26.62°) was observed as well as other weak peaks, which represented the rhombohedral graphite phase [33].

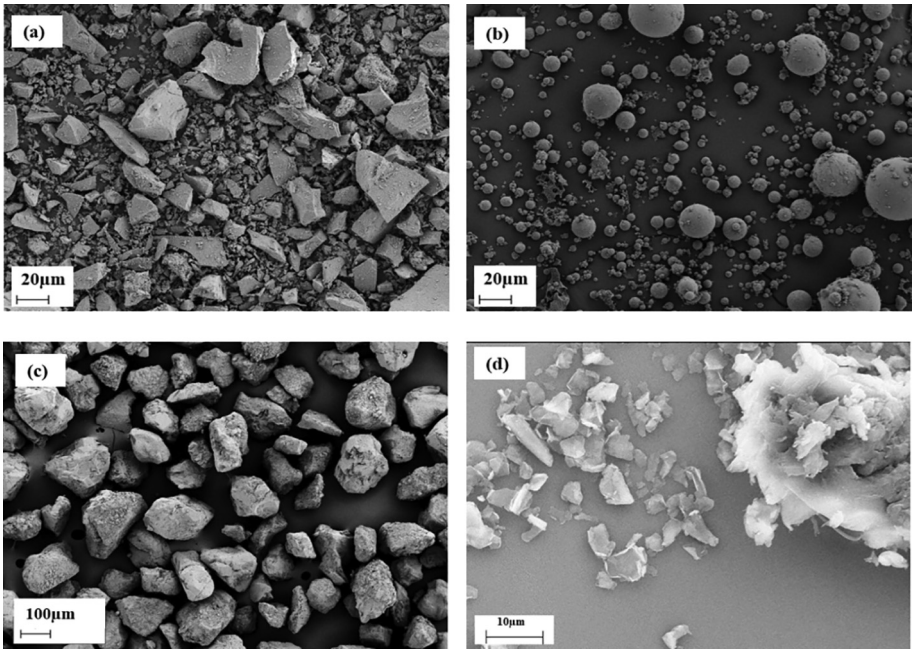

Fig. 1. Microstructure of (a) ground granulated blast furnace slag, (b) fly ash, (c) silica fume and (d) Nano-graphite platelets.

Table 1
Chemical compositions (oxides) of FA, GGBS and SF (% by weight).

	CaO	SiO_2	Al_2O_3	FeO	K_2O	Na_2O	MgO	SO_3	TiO_2
FA	3.47	52.18	24.16	9.55	3.75	1.47	1.29	3.21	1.14
GGBS	45.29	33.06	10.34	–	0.71	0.31	6.61	2.39	0.67
SF	0.35	98.37	0.19	0.08	0.28	0.20	0.15	0.19	–

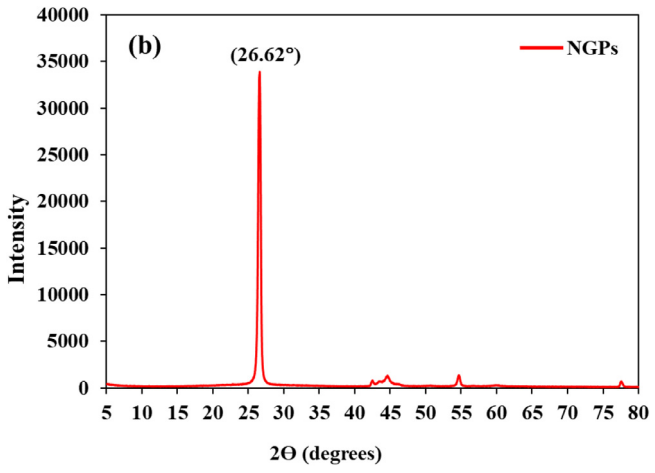

Fig. 2. XRD of as-received nano-graphite platelets.

2.2. Mixing procedure and design formulations

Six geopolymer mixes with a constant water/solid ratio of 0.4 were prepared by varying the solid components consisting of sand, FA, GGBS and SF, as shown in Table 2. Accordingly, the GGBS and SF content ranged between 15 and 35% and 5–15%, respectively, of the overall binder (FA + GGBS + SF) content, in which the amount of the activator (NaOH and Na2SiO3) content was kept constant at 18% (i.e. by weight) of the binder. For Mix 5 and 6, the decrease in GGBS and SF was accommodated for by an increase in FA content (i.e. FA content ranging from 60 to 70%). Furthermore, fine river sand was dried and sieved to obtain the particle size distribution of 0–0.5 mm and 0.5–1 mm. The river sand was added to the binder at a sand/binder ratio of 0.55, and constant size distribution of 40% of grade 0–0.5 mm and 60% of 0.5–1 mm for Mix 1, 2, 3, 5, 6 and interchanged to 40% of grade 0.5–1 mm and 60% of grade 0–0.5 mm for Mix-4. To produce the mixtures, the solid ingredients were mixed in the dry state for 2 min with a planetary mixer (Kenwood, Germany) at 250 rpm, forming the precursor materials. The sodium hydroxide and sodium silicate (NaOH and Na_2SiO_3) solutions were mixed for a period of 5 min at 700 rpm, forming the alkali-activator. This solution was slowly added to the precursor materials, and the resulting paste was stirred for 2.5 min at 250 rpm, followed by 2.5 min at 450 rpm. The mixing continued until a homogeneous geopolymer mixture was obtained. The geopolymer was then placed in 40 × 40 × 160 mm prismatic moulds for the traditionally casted samples or poured in 3D printer hopper for the printing process. The casted and printed specimens were placed immediately in a temperature and humidity controlled environmental chamber at 60 °C for 24 h. Subsequently, the samples were left in a laboratory condition of 20 °C for curing until the test age.

2.3. NGP/Geopolymer sample preparation

Some researchers have used different types of reinforcing additives in cementitious composites to improve the mechanical performance of both conventionally casted and 3D printed cementitious parts [25]. However, the incorporation of NGPs in geopolymers has been only examined for the traditionally casted samples. Based on the significant improvements as results of these materials in the casted cementitious composites [27,34], in this

Table 2
Mix design formulations.

Mixture Name	Binder			Additive NGPs Wt% (of geopolymer)	Aggregate		Na_2SiO_3: NaOH ratio
	FA Wt%	GGBS Wt%	SF Wt%		0–0.5 mm Wt%	0.5–1 mm Wt%	
Mix-1	60	35	5	–	40	60	2:1
Mix-2	60	30	10	–	40	60	2:1
Mix-3	60	25	15	–	40	60	2:1
Mix-4	60	25	15	–	60	40	2:1
Mix-5	65	20	15	–	40	60	2:1
Mix-6	70	15	15	–	40	60	2:1
M4-nG-0.1	60	25	15	0.1	60	40	2:1
M4-nG-0.3	60	25	15	0.3	60	40	2:1
M4-nG-0.5	60	25	15	0.5	60	40	2:1
M4-nG-1	60	25	15	1	60	40	2:1

study the role of NGPs incorporated in geopolymers for improving the 3D printed samples is investigated.

NGPs/Geopolymer composites were prepared in the following two steps: 1) the NGP powder was sonicated by means of ultrasonic processor (VC 750, Sonics and Materials, USA) in the mixing water for 30 min to homogeneously disperse the NGPs and separate the flakes by reducing the Van der Waals bonding between the platelets to produce individual platelets. 2) Then, the NGPs dispersed solution was added to the alkali activators and mixed vigorously via high-shear mixer device for 5 min. The Nano-graphite/alkali activator suspension was then added to the dry mixtures to obtain NGP/Geopolymer composites. As shown in Table 2, four different dosages of NGPs (i.e. 0.1%, 0.3%, 0.5%, and 1% by the weight of geopolymer) were incorporated in the selected mixture (i.e. Mix4) to assess the improvements in the mechanical performance of the printed parts compared to that of traditionally casted control sample without Nano-graphite. It is worth mentioning that 1% NGP was the maximum quantity that could be dispersed in the required water without agglomeration. Fig. 3 shows all the characterization, experimental techniques and research strategy employed in this study.

In general, the presence of NGPs with high elastic modulus, tensile strength, and specific surface area (i.e. approximately 1TPa, 130 GPa, and 402 m^2/g, respectively) makes them ideal as a 2D nanofiller within the geopolymers. Due to the ceramic-like nature of geopolymers, the cracks can be generated in any random direction and propagate throughout the matrix. The external loads (i.e. compressive or flexural) transfer to the high elastic modulus NGPs, which absorb excess energy and pass the energy uniformly throughout the matrix [35]. Since the NGPs are dispersed randomly and uniformly, they prevent the cracks propagation in any direction, which is attributed to the crack bridging, blocking, and shielding phenomenon [27].

2.4. Printing system and process parameters

In this study, a gantry-type extrusion-based 3D printer is used, shown in Fig. 4. The 3D printer was equipped with an auger extruder with a 20 mm circular nozzle. The motion speed was selected to be 20 mm/s. The nozzle standoff distance and the thickness of each printed layer were selected to be 10 mm. For all the mixtures in this study, a rectangular-shaped specimen was printed and then cut to the prisms with the dimensions of 160 × 40 × 40 mm in order to keep it consistent with the casted specimens.

2.5. Characterisations and testing procedures

2.5.1. Flow table test

Flow table test was carried out in accordance with BS EN 1015-3:1999. The fresh geopolymers were left on the flow table test for the duration of 15 min. The readings for the diameter of the flow was taken at 0, 5 and 15 min.

2.5.2. Setting time test

In this research, the Vicat needle test was assessed to evaluate the setting time of the cementitious mixtures following ASTM C191-08 and BS EN480-2:2006.

2.5.3. Open time test

The open time term refers to the period in which the fresh material paste shows suitable workability for printing. Several researches utilized Vicat, slump or rheology tests over specific interval times to approximately estimate the open time of the fresh pastes [36–38]. In this research, the actual open time was measured by printing the simple line of 250 mm × 24 mm after the rest time intervals of 5 min. The open time was mainly considered as the time that the discontinuity of the printed line occurred.

2.5.4. Shape retention test

Six layers were printed to evaluate the shape retention of each geopolymer mixture. After about 60 min, the height of each layer was measured [39]. For the sake of accurate and digital measurements, ImageJ software was employed to get the exact height measurements of each layer analysed through footages obtained from printing process for each mix.

2.5.5. Rheology test

The rheology behaviour of fresh geopolymers were obtained by means of KinexusLab + rheometer (Malvern Instruments Ltd., UK) equipped with the rSpace software (Malvern Panalytical Ltd, UK) immediately after mixing. The shear stress (τ) and apparent viscosity (η) were recorded while the shear rate (γ) was increased from 0.1 s^{-1} to 30 s^{-1} over 22 speed intervals. As several parameters such as shear rate range, chemical additives, mix designation, activator-binder ratio can alter the rheological behaviour of geopolymers, several fitting models have been proposed [40]. In this study, two fitting models, i.e. Bingham model (BM) and Herschel–Bulkley model (HB) were used to evaluate the values of rheology parameters. However, it was evident that the fitting parameters were not accurate enough. Therefore, according to the pseudoplastic behaviour and non-Newtonian nature of fresh geopolymer mixtures in addition to improving the accuracy of HB model by being able to add a linear part [41], modified-Bingham model (MBM) (see Eq. (1)) was adopted to accurately fit the shear stress vs shear rate curves and the rheology parameters, i.e. Yield shear stress (τ_0) and plastic viscosity (η_p) were extracted [17,31,42,43].

$$\tau = \tau_0 + \eta_p \cdot \gamma + c\gamma^2 \quad (1)$$

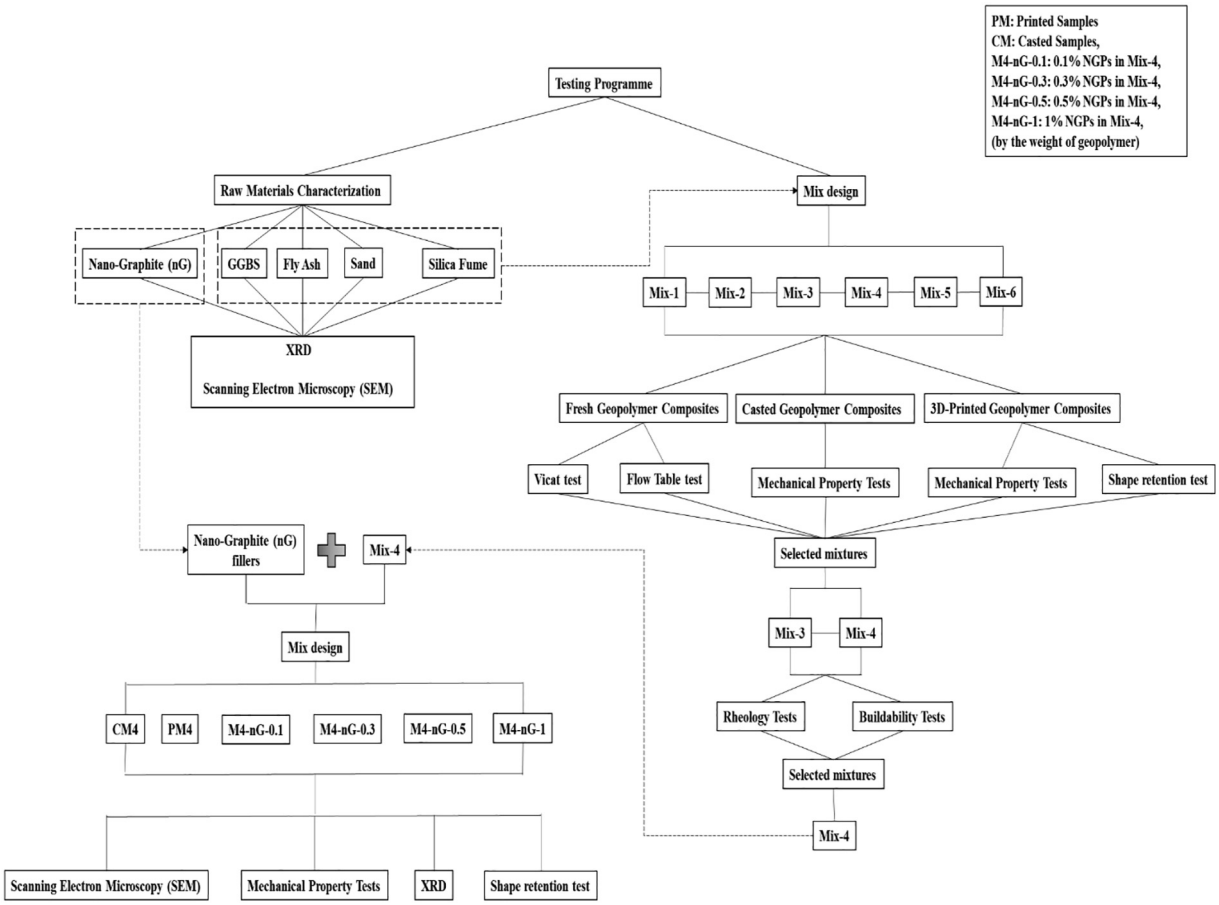

Fig. 3. Experimental framework and testing programme used in this study.

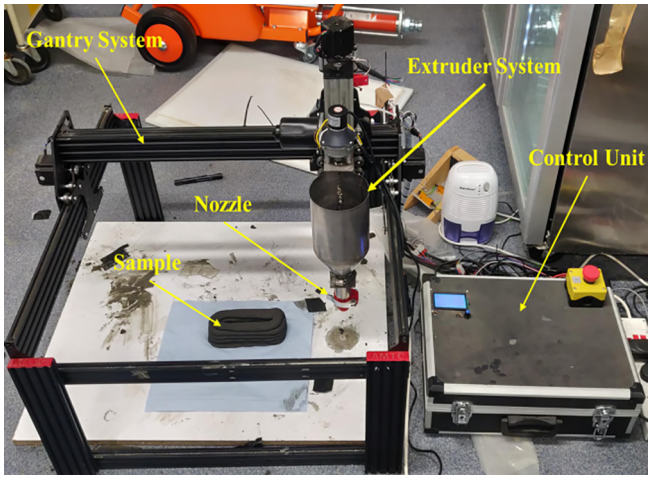

Fig. 4. Extrusion based 3D printer.

As reported by Chen et al. (2018), the rheology parameter values required for 3D printing process is different from that of conventionally casted specimens. In this regard, the suitable mixture for 3D printing should have low yield stress and sufficient flowability to be well-extruded through the nozzle as well as high viscosity at the same time to retain the shape straight after the deposition from nozzle [44]. All the obtained rheology values were aligned and in range with the values reported for geopolymers by several articles [45–48].

2.5.6. Mechanical test

The flexural and compressive strength of each sample was tested after 7 days in accordance with BS EN 196-1:2016 or EN 196-1 using a 150kN universal testing machine (Instron 5960, United Kingdom) at a constant loading rate of 1 mm/min. The values of compressive and flexural stress are the average of values obtained from three specimens in which the loading direction is perpendicular to the printing path.

2.5.7. Microstructural analysis

Microstructural studies were performed using SEM (Supra 35VP, Carl Zeiss, Germany)) equipped with Energy dispersive spectroscopy (EDS) analyser (EDAX, U.S.A). Energy dispersive spectroscopy (EDS) and secondary electron images were collected from broken portions of specimens in a flexural strength test. To prepare the specimens, at least 10 samples of approximately 10 mm^3 were gold-coated and observed by SEM to have a reliable statement about the morphology of geopolymer composites.

3. Results and discussion

3.1. Fresh properties of geopolymers

The fresh properties of cementitious-based materials are the most important aspect for successful 3D printing. The characteristics of aggregates such as size, shape, gradation and surface textures, as well as its volume fraction can significantly influence the fresh properties of geopolymers, e.g. flow-ability, workability and shape stability [49]. Fig. 5 shows the flow-ability of the

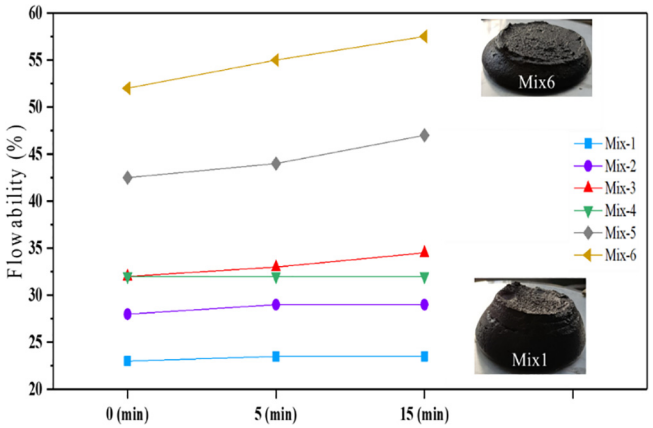

Fig. 5. Flow table test results of different geopolymer mixes.

geopolymers studied in this investigation using the flow table test. The lowest and the highest flow-ability was achieved by Mix-1 and Mix-6, with an initial (i.e. 0 min) flow-ability of 23% and 52%, respectively. The results revealed that, by decreasing the GGBS content and replacing it with the other binder components (i.e. fly ash and silica fume), the flow-ability of the mixture increases considerably. With the decrease of GGBS content (i.e. from 35 wt % to 15 wt%), the cohesiveness of the paste was reduced due to the reduction in angular shape particle content and substitution by rounded and spherical shape particles (see Fig. 1). Thus, the additional amount of rounded and spherical shape particles is expected to serve as a lubricant leading to an increase in flow-ability [49–51]. A larger variation of aggregate particle distribution (Mix-3: 40% sand of 0–0.5 mm and 60% sand of 0.5–1 mm) has been incorporated into the design formulation of this study and compared with the smaller aggregate size (i.e. Mix-4: 60% sand of 0–0.5 mm and 40% sand of 0.5–1 mm). The aggregate size reduction, from Mix-3 to Mix-4, led to increased cohesiveness and reduced flow-ability whilst maintaining good shape stability. The flow-ability reduction for Mix-4 occurs due to higher specific area of small aggregates, which increase the moisture absorption and friction between the aggregates in the mixture [52,53]. These results are fully aligned with the results obtained in rheology measurements (see Fig. 9 and Table 4).

3.1.1. Setting time and open time behaviour of geopolymers

According to several studies [51,54–56], alkaline solution and binder type have a significant influence on the setting and open time of the geopolymers. Moreover, Elyamany et al. (2018) study revealed that increasing the slag content as a main source of calcium leads to achieving higher setting time [55]. As reported by several authors, the initial setting time and open time of cementitious materials are directly related to each other [36,57,58], which is desirable and essential for large-scale 3D printing process [55]. In this study, in order to adjust the best setting and open time for 3D printing, the GGBS content has been changed while the alkaline solution ratio remained constant. The influence of GGBS on setting time, by means of Vicat tests have been investigated (Fig. 6a). It can be seen that by replacement of GGBS with other binders (i.e. fly ash and silica fume), the setting time of the mixtures has considerably increased from 12 to 47 min, for Mix-1 to Mix-6, respectively. The same relationship was also observed for the open time test (Fig. 6b and c), the open time gradually increased from 10 to 35 min for Mix-1 to Mix-6, respectively. The aforementioned behaviour of geopolymers may be due to the higher dosage of GGBS in geopolymers, which contributes to a denser structure, and subsequently leads to rapid setting times. A

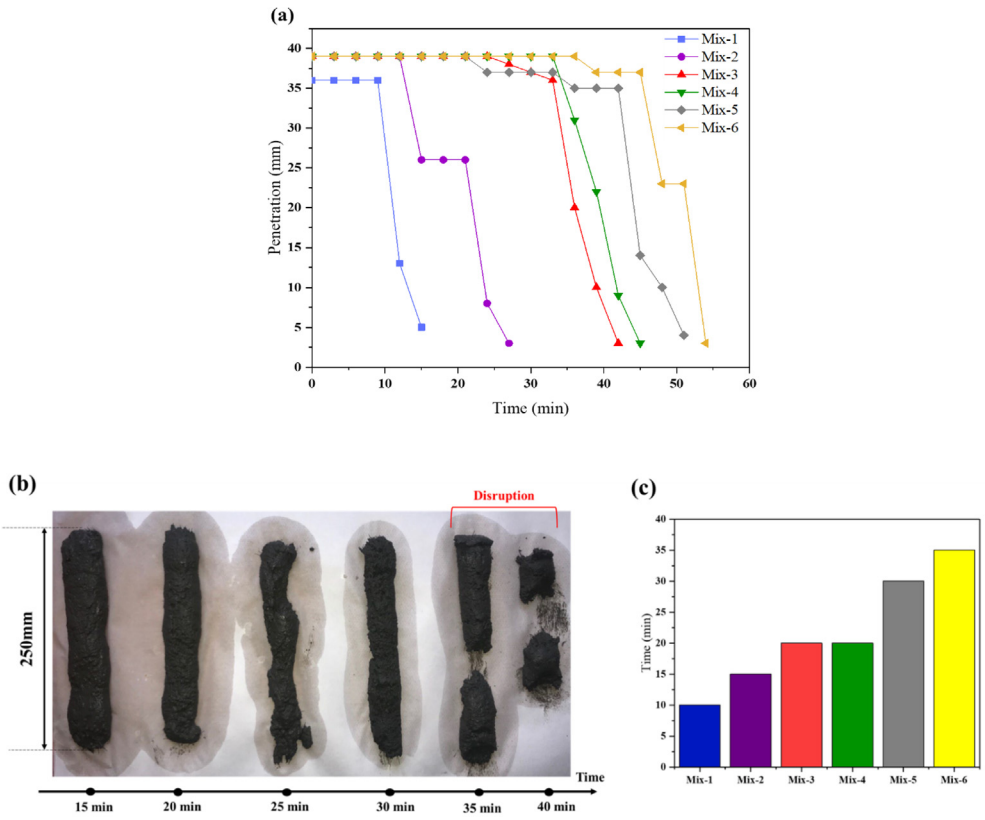

Fig. 6. (a) Setting time and (b) and (c) open time results of geopolymers.

similar trend was observed by [51,59] study, which concluded that higher dosage of GGBS leads to increasing in CaO content of the mixtures. High CaO content in GGBS may help to form C–S–H gel along with the 3D stable silico-aluminate structure by the geopolymeric reaction at an early age. By comparing the setting and open time of Mix-3 (27 and 20 min) and Mix-4 (33 and 20 min), it can be seen that sand grade size does not have considerable influence on the setting and open time of mixtures, i.e. 6 min difference in setting time and equal open time between Mix-3 and Mix-4.

3.1.2. Shape retention

The shape retention test is important as this parameter for 3D printing of cementitious materials can provide a qualitative measurement to evaluate the shape stability of 3D printed layers, therefore is an indirect method for measuring the structural build-up. Each subsequent layer's weight on the first printed layer was evaluated to assess the shape stability of the fresh mix. The visual measurement was combined with the picture processing software to quantify and increase the accuracy of the results. This measurement focuses on two interlinked parameters. First, the height difference between the first printed layer and the last printed layer was assessed, i.e. the lower the difference, the better shape retention. Second, the first layer's height after the deposition of five subsequent layers printed was measured. Each printed layer's height was calculated employing Fiji ImageJ software. Each mixture was printed in six layers to capture a high-quality image and carry out the calculations. The image pixels were then calibrated using a scale, which was placed exactly next to the printed samples. Subsequently, the height of each layer after deposition from the nozzle was calculated automatically by converting the number of image pixels to millimetres. For instance, Mix-4 was printed for six subsequent layers, the high-quality image was captured and then imported to the Fiji ImageJ software. After scale adjustment and pixels calibration, the software measured each layer's height. The fit curve was then plotted to indicate the shape retention of each geopolymer mix, see Fig. 7. The results show that Mix-4 has better shape retention compared to the other geopolymers in terms of first layer height (i.e. 7.5 mm) and its difference between the first layer and last layer height (i.e. 14.5 – 7.5 = 7 mm). It means that this mixture can maintain its shape during the deposition of the upper subsequent layers. This could be due to the setting time and open time (see Fig. 6a–b) of Mix 4 as measures previously, i.e. 33 and 20 min respectively, which allows this mixture to exhibit superior shape retention compared to the other geopolymer mixtures.

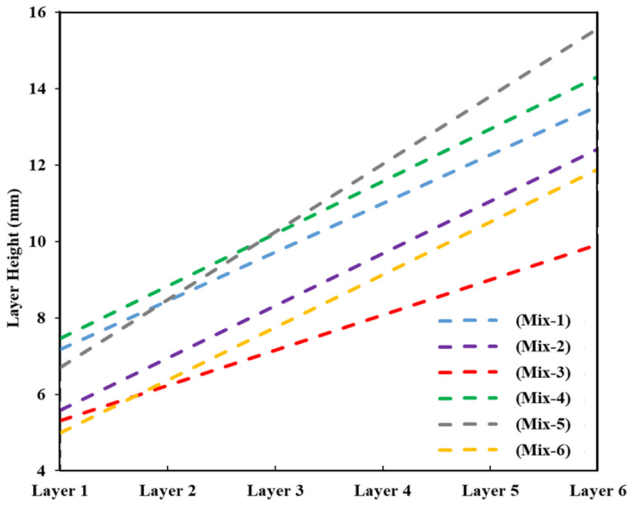

Fig. 7. Each layers' height after the deposition of subsequent layer.

3.2. Mechanical properties of geopolymers

It is important to bridge the mechanical performance gap between the conventional casted geopolymer specimens with the 3D printed counterparts. Mechanical properties and their link to the density of each geopolymer mix has been evaluated in this section. Fig. 8a–c presents the various geopolymeric mix designs and their corresponding mechanical performance for both printed and conventionally casted samples. The difference between the casted and printed specimens has been compared by means of compressive and flexural strength measurements. The comparison between the flexural strength of 3D printed and casted specimens (Fig. 8a) in the perpendicular direction of load revealed that, for all geopolymers except Mix-3, the flexural strength of 3D printed samples is lower than the casted samples. The flexural strength of 3D printed Mix-3 (i.e. PM3), unlike the other compositions, was 12% higher than that of the Casted Mix-3 (i.e. CM3). This may be because the bottom printed layers govern the flexural strength where the maximum tensile stress takes place. As it can be seen in Fig. 7, Mix 3 had a well-compacted bottom layers due to the weight of the layers above it (approximately 5.7 mm). This leads to load capacity of the bottom layers, thereby the higher flexural strength in the perpendicular direction [60].

The density comparison between printed and casted samples are represented in Fig. 8c. For Mix-1 and Mix-2 the density of printed samples are lower than that of casted samples. This could be potentially due to the lower flow-ability and setting time of these two mixtures as observed in Figs. 5 and 6. The low setting time of the geopolymers can impede the compaction during the extrusion process, resulting in lower densification and higher porosity compared with traditionally casted samples [61]. For all the other mixtures, the density of 3D printed samples is higher than their casted counterparts. This could be associated with the higher flow-ability and setting time of fresh mixtures resulting in compaction and densification during and after the printing process. Panda et al. (2018) also reported the density enhancement (i.e. 2050 kg/m^3 for geopolymer 3D printed parts with respect to 1500 kg/m^3 for casted samples) due to the application of high pressure during the extrusion process [62].

In Fig. 8b it is evident that the compressive strength of casted samples has a descending trend from 67 MPa with a coefficient of variation (CoV) of 7% for Mix-1 to 44 MPa (CoV of 6.2%) for Mix-6 (34% decrease). This may be due to the fact that higher dosage of GGBS in the geopolymer contributes to an increase in calcium aluminosilicate (C-A-S-H) and sodium aluminosilicate (N-A-S-H) content and thus, form a denser structure (See Fig. 8c, casted samples density) to gain higher strength, which, is in agreement with the observed results by Xie et al. (2019) [59]. It can be seen that all the casted samples demonstrate greater compressive strength compared to their 3D printed counterparts.

3.3. NGP/Geopolymer composites and their characterisation

Extrudability, shape retention and buildability are all interlinked and dependent on rheology of geopolymeric mixtures [58]. To achieve adequate extrudability, the geopolymer paste has to be reasonably flow-able to be extruded out of the 3D-printer nozzle. On the other hand, the higher flow-ability translates into insufficient shape retention properties of the mix (e.g. losing shape with minimum applied pressure from the above layers). Therefore, there is a direct influence on the buildability and a limit on the number of printed layers. Investigating and selecting the exact balance between all three parameters through optimizing

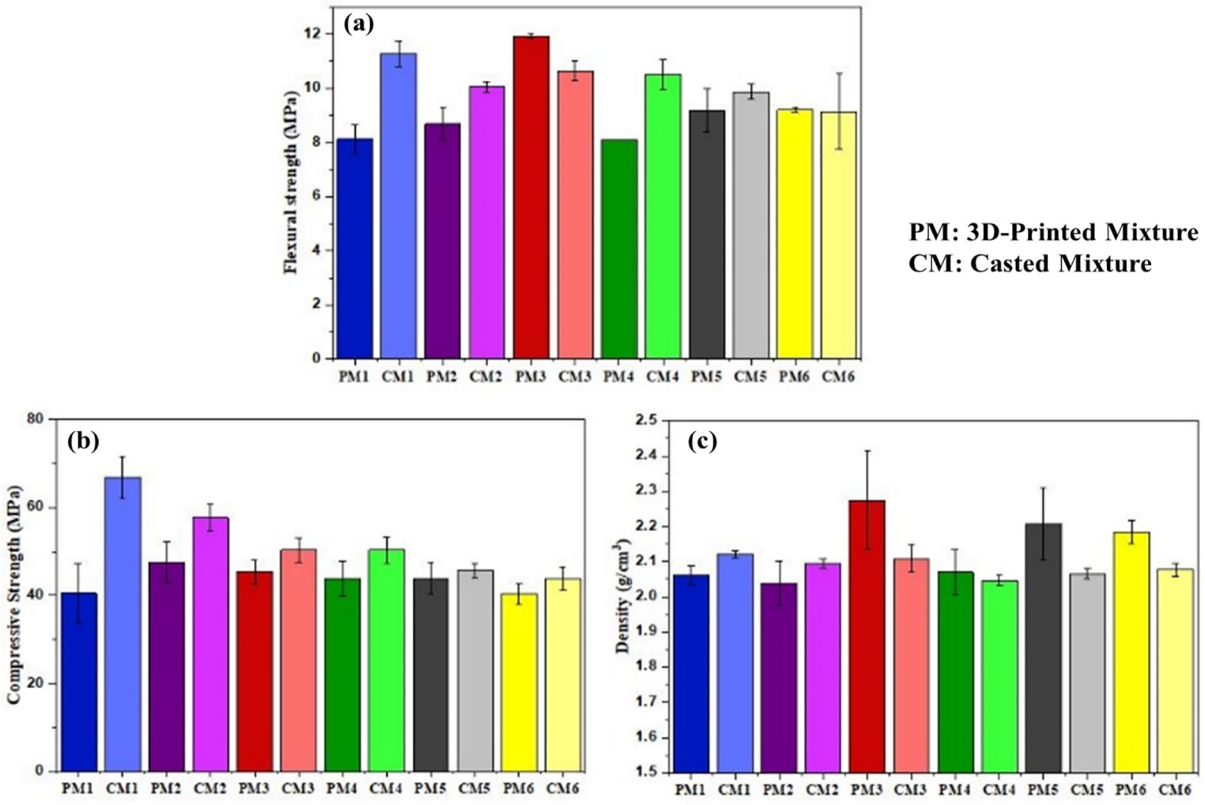

Fig. 8. Density and mechanical properties of printed (PM) and casted (CM) geopolymers, (a) flexural strength, (b) compressive strength, and (c) density.

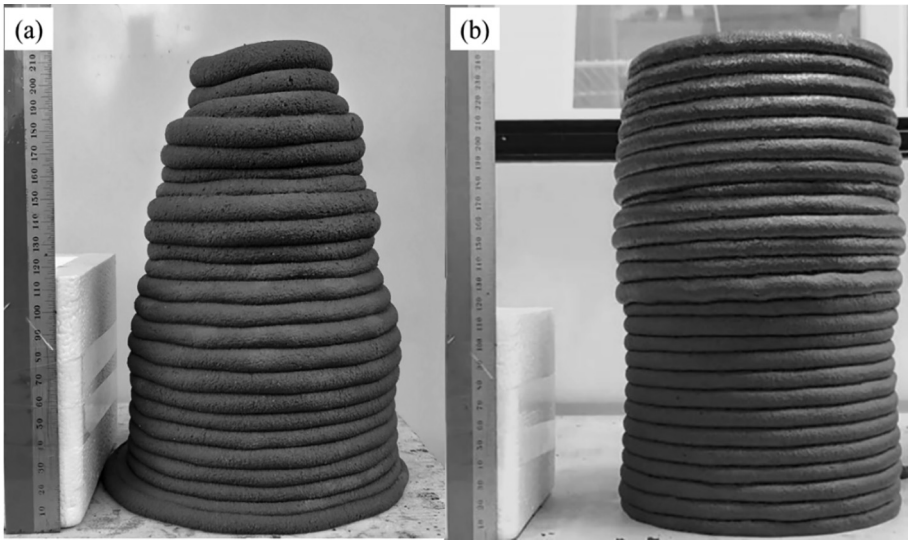

Fig. 9. Buildability of 20 layers for (a) Mix-3 and (b) Mix-4.

the mix design is essential to ensure adequacy in 3D printing process. According to the previous test results obtained from workability, setting time, shape retention and mechanical property assessments, Mix-3 and Mix-4 demonstrated more reasonable printing performance and mechanical properties. Therefore, buildability and rheology tests were carried out to select the superior mixture for the incorporation of NGPs as fillers to evaluate if their addition can improve the mechanical properties of 3D printed geopolymer mixtures. The buildability test was carried out for both mixtures, Mix-3 and Mix-4, by printing 25 layers (i.e. 30 cm). As demonstrated in Fig. 9a, for Mix-3, after ten layers of printing, the geometry experienced a considerable distortion and collapse while for Mix-4 (Fig. 9b) the selected geometry was printed successfully with an adequate shape without any apparent distortion.

The buildability comparison between Mix-4 and Mix-3 was supported by the rheology results. As it can be seen in Fig. 10b, Mix-3 demonstrates a lower apparent viscosity to that of Mix-4. The yield shear stress and plastic viscosity results (Fig. 10a and Table 3) also showed that Mix-3 had lower yield shear stress and plastic viscosity (i.e. 13.43 Pa and 6.82 Pa·s) compared to that of

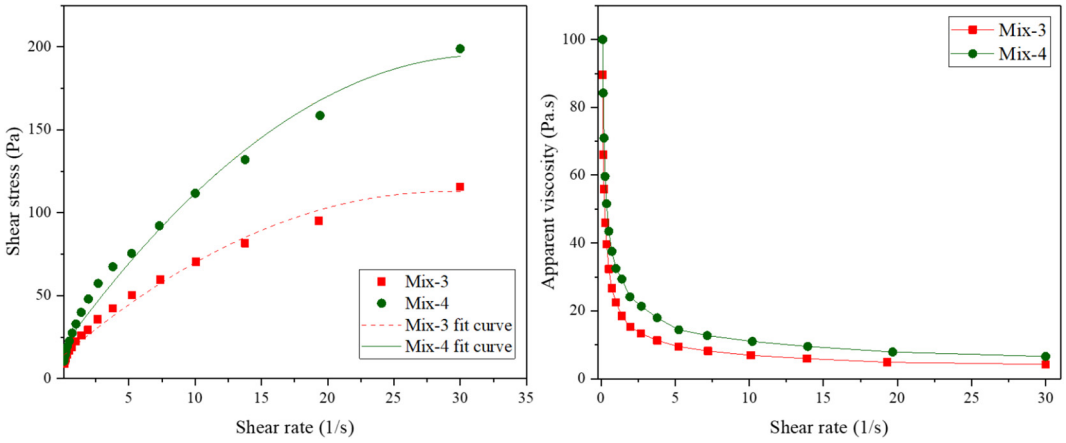

Fig. 10. Rheology measurements of Mix-3 and Mix-4 (a) shear stress and (b) viscosity.

Table 3
Rheological properties of Mix-3 and Mix-4.

Sample name	τ_0 (Pa)	η_p (Pa·s)	Correlation coefficient (R2)
Mix-4	18.58	11.03	0.9862
Mix-3	13.43	6.82	0.9864

Table 4
Rheological properties of Mix-4 with different NGP ratios.

Sample name	τ_0 (Pa)	η_p (Pa·s)	Correlation coefficient (R^2)
Mix-4	18.585	11.03	0.9862
M4-nG-0.1	16.144	10.53	0.9949
M4-nG-0.3	17.994	11.11	0.996
M4-nG-0.5	11.949	6.61	0.9929
M4-nG-1	36.414	17.27	0.9751

Mix-4 (i.e. 18.58 Pa and 11.03 Pa·s). The higher rheology values of Mix-4 could be attributed to the smaller aggregate size (i.e. 60% of 0–0.5 mm sand) with higher specific surface area of Mix-4, which required higher activator solution demand to flow. The effect of small aggregate size on the rheology of geopolymer pastes has been previously investigated, where it was proven that the presence of aggregates with high specific surface area increase the rheology parameters [52,53]. The poor buildability of Mix-3 could be due to (i) lower open time for printing of Mix-3 in comparison to Mix-4, which can cause cold joint between the layers during the printing, as well as, (ii) lower yield shear stress of Mix-3, which shows its lower capacity to bear the deposited layers weight [58].

In order to further investigate shape stability of Mix-4, the dynamic shape retention of Mix-4 during the deposition of layers was carried out. In this examination, the height reduction of first layer after the deposition of each upper layer was measured using ImageJ software and plotted in Fig. 11. The results indicate after 15 layers (approximately 18 min of printing) maximum height reduction of 8.7 mm (from 15.2 mm to 6.5 mm) for the first layer was observed, after which, the first layer was set and its height reduction stopped. The superior shape retention of the first deposited layer can serve as a base to hold the weight of the upper layers and therefore, lead to better performance of this mixture for large-scale structure 3D printing.

In this stage of the study, Mix-4 as an appropriate mix design that satisfied the necessary requirements for 3D printing, i.e. sufficient flow-ability, buildability, shape stability and mechanical performance, was nominated to be used as a suitable feedstock for the incorporation of NGPs to assess if its mechanical properties can be further enhanced, more specifically the flexural strength.

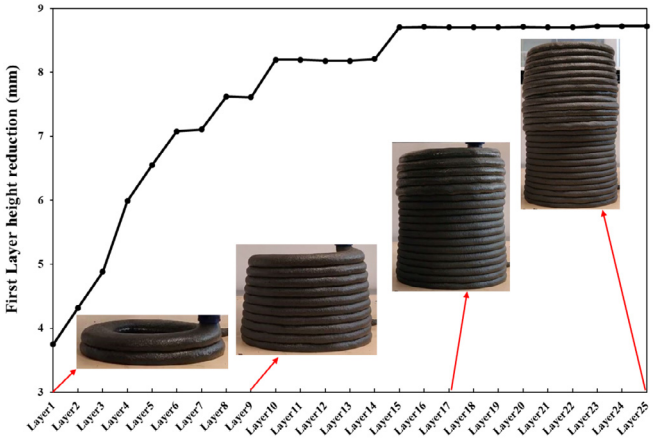

Fig. 11. Dynamic shape retention test of Mix-4 for 25 layers of printing.

3.3.1. Shape retention of NGP/Geopolymer composites

As it can be seen in Fig. 12, the addition of NGPs, in all cases, increase the shape retention of geopolymers by reducing the difference between the first and the last layer's height. The best result

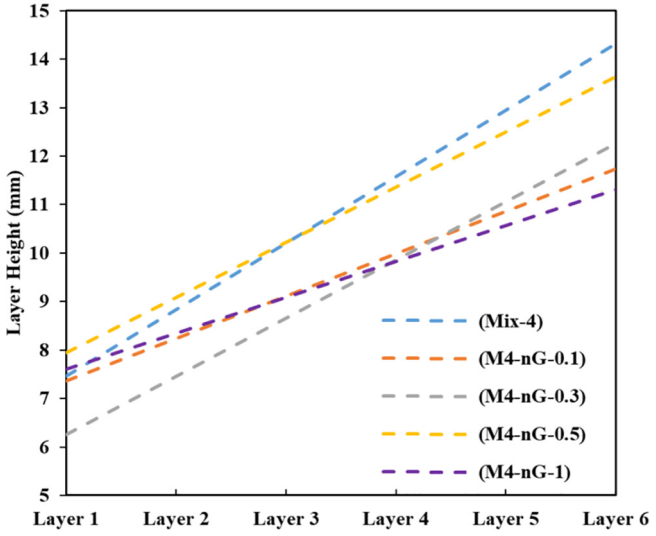

Fig. 12. Each layers' height after the deposition of subsequent layer in Mix-4 with different dosages of NGP.

was observed for the highest dosage of NGPs (i.e.1 wt% addition), where the difference between the first and last layer was measured to be approximately 3.4 mm. This is 52% lower than that of Mix-4 without NGPs (i.e. 7.1 mm). The observation can be explained by the presence of Van Der Waals forces between the Nano-graphite particles and the super sorbent characteristics of Nano-graphite particles, which leads to geopolymer's main components to be close together and hence, obtain a better shape retention [63,64]. Moreover, one other explanation could be that the additional amount of NGPs has simply made the paste more cohesive, therefore, encouraging a denser packing, which contributes to better shape retention.

3.3.2. Rheology measurements of NGP/Geopolymer composites

Fig. 13a–b and Table 4 show the influence of NGPs incorporation on the rheology of the selected mixture (i.e. Mix-4). The results demonstrate that the rheology of geopolymers are sensitive to the addition of different dosage of NGPs. In agreement with the previous studies, Meng et al. (2018) reported the same effect of NGPs on cementitious composites. The authors believed that the presence of nano-graphite particles in geopolymers could induce two conflicting effects. First, the super-sorbent characteristic of NGPs, which consume the moisture of the mixture, result in increasing the rheology values and second, the lubrication effect of NGPs in certain dosages, which decreases the rheology values [64].

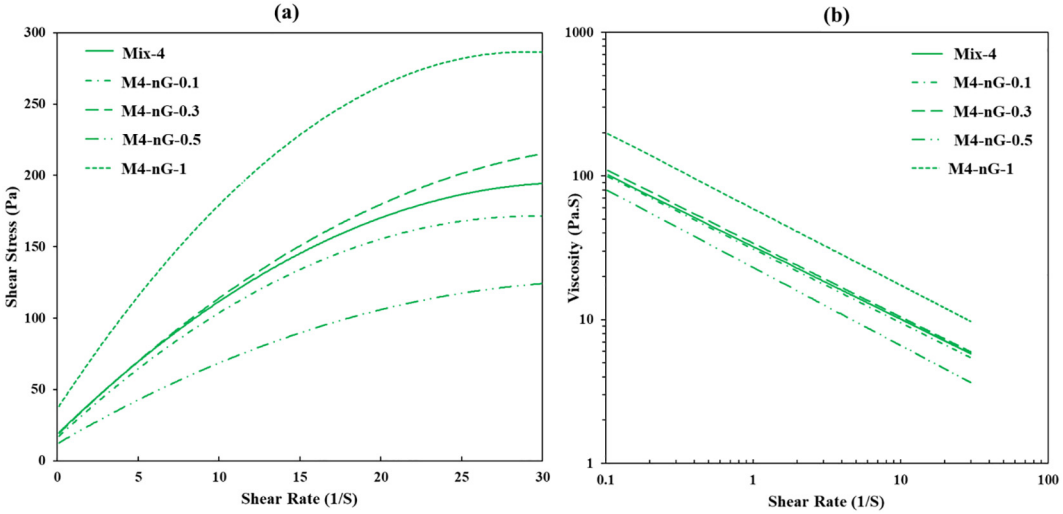

Fig. 13. Rheology measurements of Mix-4 with different NGP ratios (a) shear stress and (b) viscosity.

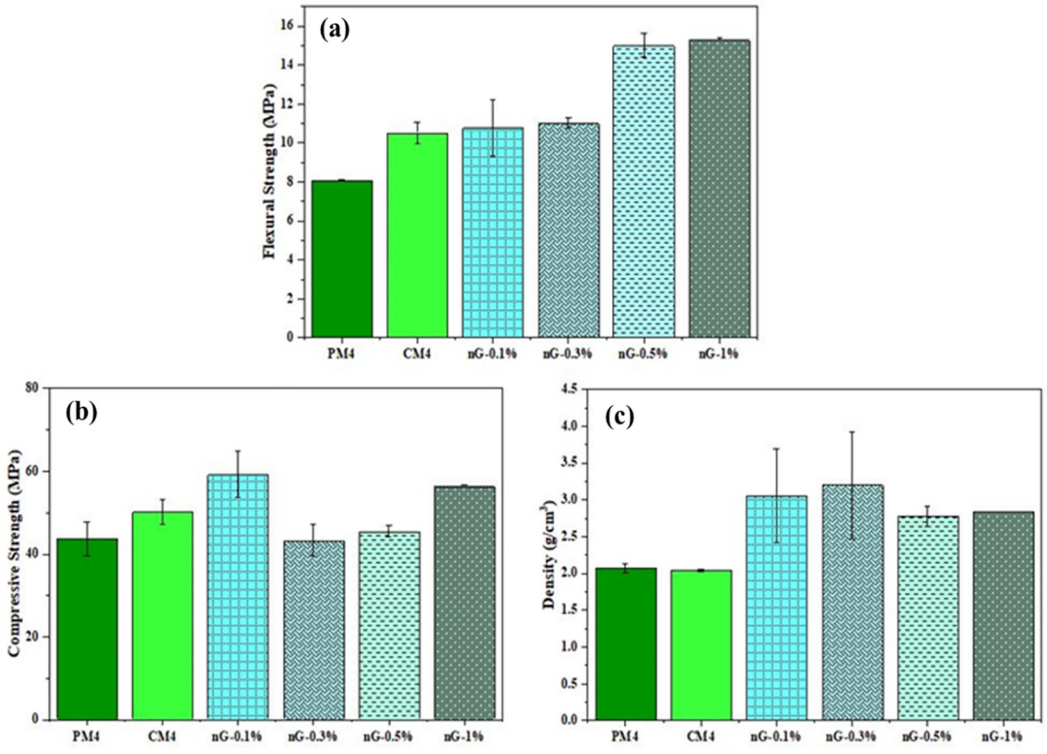

Fig. 14. Printed (PM) and casted (CM) Mix-4 with different NGP ratios (a) flexural strength, (b) compressive strength and (c) their densities.

As displayed in Table 4, the yield shear stress and plastic viscosity results showed comparable values for M4-nG-0.1 and M4-nG-0.3 to the values registered for Mix-4 without any NGPs (i.e. 18.585 Pa and 11.03 Pa·s, respectively). However, the values drastically decreased to 11.949 Pa and 6.61 Pa·s for M4-nG-0.5. This observation can be attributed to the fact that the lubrication effect of nano-graphite dominate over their thickening effect [31,64]. The addition of more nano-graphite particles (i.e. M4-nG-1) counterbalanced the lubrication effect and remarkably increased both, the yield shear stress and plastic viscosity to 36.414 Pa and 17.27 Pa·s, respectively. The apparent viscosity showed a similar behaviour to shear stress versus shear rate results. The rheology measurement results are aligned with the observations obtained in the shape retention test (see section 3.1.2). Therefore, it is worth emphasizing that the rheology measurements of fresh geopolymers are essential for predicting the printability of mixtures. In agreement with Panda et al. (2019), the comparison of the results obtained from shape retention tests and rheology measurements show that the higher yield stress and viscosity of geopolymers lead to better shape retention [58].

3.3.3. Mechanical properties of NGPs/Geopolymer composites

Mix-4 was incorporated with four different dosage of Nano-graphite platelets (i.e. 0.1%, 0.3%, 0.5% and, 1%) where the mechanical properties of each mix is represented in Fig. 14. The NGPs modified mixtures were 3D-printed and compared to that of casted Mix-4 samples without NGPs. The results revealed that the addition of NGPs progressively increases the flexural strength from 10.5 MPa (CoV of 5.3%) for the casted sample to 10.7 (CoV of 10%), 11.2 (CoV of 2.2%), 15 (CoV of 4%) and, 15.3 (CoV of 0.3%) MPa for M4-nG-0.1, M4-nG-0.3, M4-nG-0.5 and, M4-nG-1 respectively (Fig. 14a). The highest percentage increase was 46% as observed in the case of M4-nG-1.

The superior improvement in flexural strength (i.e. up to 46% with respect to the casted mix 4) is potentially attributed to the crack bridging and crack blocking caused by the presence of NGPs in geopolymer's microstructure. As it can be seen in Fig. 15, after micro-crack initiation caused by the imposed load in three point bending test, the micro-cracks tend to grow and propagate through the microstructure of geopolymers due to the stress concentration increase. Thus, as soon as the micro-cracks meet the NGPs with

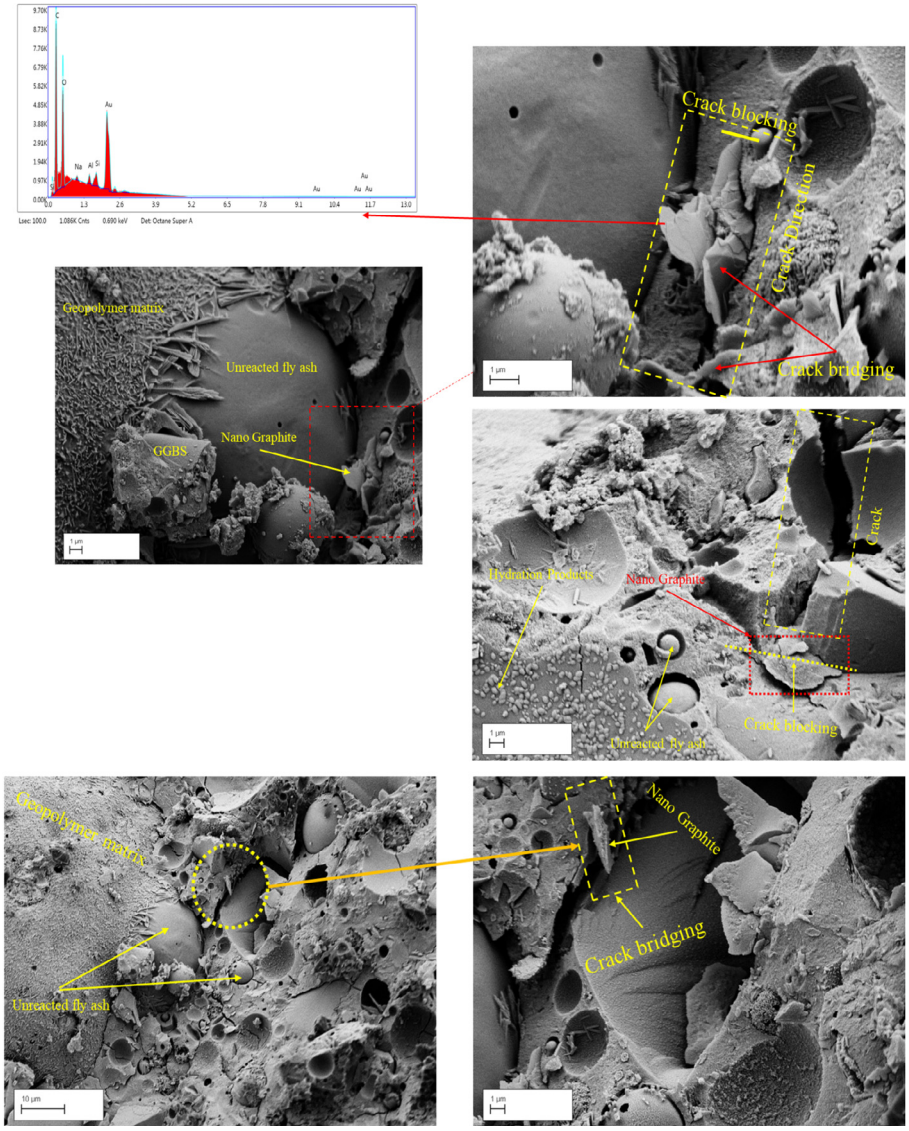

Fig. 15. The microstructural analysis of the failure zone of Mix-4 with 1% of NGPs addition.

higher elastic modulus, more energy is needed to overcome the high-energy absorbance of NGPs, thereby, increasing flexural strength. Ranjbar et al. (2015) observed a similar effect of NGPs on geopolymer samples. Their results revealed that the addition of only 1% GNPs improved the flexural and compressive strength of fly ash-based geopolymers by 216% and 144% respectively. The authors believed that the remarkable improvement in flexural strength is attributed to various toughening mechanisms of GNPs i.e. stress propagation, crack deviation, crack blocking and crack bridging [27].

Fig. 14c shows that the density was increased for all compositions and the maximum enhancement was observed for M4-nG-0.1 and M4-nG-0.3, about 3 gr/cm^3 and 3.2 gr/cm^3, respectively in comparison to 3D printed and casted samples without the addition of NGPs. The density increase is associated with better compaction during the extrusion process and the reduction of voids. The presence of NGPs induce a lubricating effect in the mix, which contributes to the compaction during extrusion by decreasing the friction between the geopolymer components.

Contrary to the flexural strength, the compressive strength of 3D printed samples modified by NGPs (Fig. 14b), first increased from 50 MPa (CoV of 6%) (for casted samples of Mix-4) to 59 MPa (CoV of 9%) for 0.1 wt% of NGPs addition. Thereupon, compressive strength was decreased to 43 MPa (CoV of 8%) and 45 MPa (CoV of 3%) for 0.3 wt% and 0.5 wt% of NGPs addition, respectively. Although the compressive strength of the aforementioned compositions decreased, they are still comparable to the value measured for the Mix-4 printed sample without NGPs (i.e. 44 MPa (CoV of 9.2%)). The addition of 1% of NGPs increased the compressive strength by 14% (i.e. from 50 MPa (CoV of 6%) for casted samples of Mix-4 to 57 MPa (CoV of 0.6%)). Therefore, it can be concluded that the incorporation of 1% NGPs will exhibit better results on flexural, compressive strength and density.

4. Conclusions

The main objective of this study was to first, investigate the fresh and hardened properties of six different geopolymers suitable for 3D printing process. Then, the flow-ability, rheology behaviour and mechanical properties of the selected geopolymer mixture containing 0.1 wt%, 0.3 wt%, 0.5 wt%, and 1 wt% of NGPs were evaluated. The actual reinforcing mechanism of NGPs in the printed samples was elucidated by microstructural analysis and crystallinity improvements. The following conclusive statements were drawn from this investigation.

The flow-ability behaviour of fresh geopolymers including setting and open time reduce with a higher dosage of GGBS in the binder.

Due to the better setting and open time, the superior shape retention was observed for Mix-4 compared to the other geopolymers.

The presence of Van Der Waals forces between the Nano-graphite particles and the super sorbent characteristics of NGPs increased the shape retention of geopolymer. The best result was observed for the highest dosage of NGPs in Mix4 (i.e. M4-nG-1%), which was 52% lower than the value registered for Mix-4 without NGPs.

The rheology measurements indicated that the addition of 0.3% and 1% Nano graphite in Mix-4 decrease the workability due to the thickening effect, however, by addition of 0.1% and 0.5% Nano graphite the lubrication effect dominated over the thickening phenomenon and the workability was increased compared to plain Mix 4.

The mechanical property of Mix 4 with 1% addition of NGPs exhibited the highest improvement due to the toughening mechanism i.e. stress propagation, crack deviation, crack blocking and crack bridging generated by the presence of NGPs.

The developed 3D printable geopolymer mix reinforced with Nano additives in this study could present new area of research for further optimising the printable feedstock and pilot scale manufacturing of mechanically robust building blocks.

CRediT authorship contribution statement

Mehdi Chougan: Formal analysis, Writing - original draft. **Seyed Hamidreza Ghaffar:** Conceptualization, Methodology, Supervision, Writing - review & editing. **Mohammad Jahanzat:** Data curation. **Abdulrahman Albar:** Data curation. **Nahzatullah Mujaddedi:** Data curation. **Rafiq Swash:** Writing - review & editing.

Declaration of Competing Interest

The authors declare that they have no known competing financial interests or personal relationships that could have appeared to influence the work reported in this paper.

References

[1] S. Ghaffar, P. Mullett, Commentary: 3D printing set to transform the construction industry, (2018) 1–2.
[2] S. Hamidreza, J. Corker, M. Fan, Automation in construction additive manufacturing technology and its implementation in construction as an eco-innovative solution, 93 (2018) 1–11. https://doi.org/10.1016/j.autcon.2018.05.005.
[3] M. Xia, J. Sanjayan, Method of formulating geopolymer for 3D printing for construction applications, JMADE 110 (2016) 382–390, https://doi.org/10.1016/j.matdes.2016.07.136.
[4] B. Zareiyan, B. Khoshnevis, Automation in construction interlayer adhesion and strength of structures in contour crafting - effects of aggregate size, extrusion rate, and layer thickness, Autom. Constr. 81 (2017) 112–121, https://doi.org/10.1016/j.autcon.2017.06.013.
[5] T. Marchment, J. Sanjayan, M. Xia, Method of enhancing interlayer bond strength in construction scale 3D printing with mortar by effective bond area amplification Method of enhancing interlayer bond strength in construction scale 3D printing with mortar by effective bond area amplification, Mater. Des. 169 (2019), https://doi.org/10.1016/j.matdes.2019.107684 107684.
[6] B. Panda, S.C. Paul, N. Ahamed, N. Mohamed, Y. Wei, D. Tay, M.J. Tan, Measurement of tensile bond strength of 3D printed geopolymer mortar, Measurement 113 (2018) 108–116, https://doi.org/10.1016/j.measurement.2017.08.051.
[7] J. Davidovits, S. Quentin, GEOPOLYMERS Inorganic polymerie new materials, 37 (1991) 1633–1656.
[8] P. Duxson, J.L. Provis, F. Si, Designing precursors for geopolymer cements, 3869 (2008) 3864–3869. https://doi.org/10.1111/j.1551-2916.2008.02787.x.
[9] J. Xie, O. Kayali, Effect of superplasticiser on workability enhancement of Class F and Class C fly ash-based geopolymers, Constr. Build. Mater. 122 (2016) 36–42, https://doi.org/10.1016/j.conbuildmat.2016.06.067.
[10] A. Nazari, J.G. Sanjayan, Synthesis of geopolymer from industrial wastes, J. Clean. Prod. 99 (2015) 294–304, https://doi.org/10.1016/j.jclepro.2015.03.003.
[11] B. Panda, S.C. Paul, L.J. Hui, Y. Wei, D. Tay, M.J. Tan, Additive manufacturing of geopolymer for sustainable built environment, 167 (2017). https://doi.org/10.1016/j.jclepro.2017.08.165.
[12] A. Mehta, R. Siddique, An overview of geopolymers derived from industrial by-products, 127 (2016) 183–198. https://doi.org/10.1016/j.conbuildmat.2016.09.136.
[13] W. Zhou, C. Yan, P. Duan, Y. Liu, Z. Zhang, X. Qiu, D. Li, A comparative study of high- and low-Al2O3 fly ash based-geopolymers: the role of mix proportion factors and curing temperature, JMADE 95 (2016) 63–74, https://doi.org/10.1016/j.matdes.2016.01.084.
[14] G.M. Zannerni, K.P. Fattah, A.K. Al-Tamimi, Ambient-cured geopolymer concrete with single alkali activator, Sustain. Mater. Technol. 23 (2020) e00131, https://doi.org/10.1016/j.susmat.2019.e00131.
[15] G. Habert, J.B. D'Espinose De Lacaillerie, N. Roussel, An environmental evaluation of geopolymer based concrete production: reviewing current research trends, J. Clean. Prod. 19 (2011) 1229–1238, https://doi.org/10.1016/j.jclepro.2011.03.012.
[16] B. Nematollahi, P. Vijay, J. Sanjayan, A. Nazari, M. Xia, V.N. Nerella, V. Mechtcherine, Effect of polypropylene fibre addition on properties of geopolymers made by 3D Printing for, (2018). https://doi.org/10.3390/ma11122352.

[17] B. Zhu, J. Pan, B. Nematollahi, Z. Zhou, Y. Zhang, J. Sanjayan, Development of 3D printable engineered cementitious composites with ultra-high tensile ductility for digital construction, Mater. Des. 181 (2019) 108088, https://doi.org/10.1016/j.matdes.2019.108088.

[18] M. Hambach, D. Volkmer, Properties of 3D-printed fi ber-reinforced Portland cement paste, Cem. Concr. Compos. 79 (2017) 62–70, https://doi.org/10.1016/j.cemconcomp.2017.02.001.

[19] F.P. Bos, E. Bosco, T.A.M. Salet, Ductility of 3D printed concrete reinforced with short straight steel fibers, 2759 (2019). https://doi.org/10.1080/17452759.2018.1548069.

[20] J.D. Ríos, C. Leiva, M.P. Ariza, S. Seitl, H. Cifuentes, Analysis of the tensile fracture properties of ultra-high-strength fiber-reinforced concrete with different types of steel fibers by X-ray tomography, Mater. Des. 165 (2019) 107582, https://doi.org/10.1016/j.matdes.2019.107582.

[21] B. Nematollahi, M. Xia, P. Vijay, J.G. Sanjayan, in: Properties of Extrusion-Based 3D Printable Geopolymers for Digital Construction Applications, Elsevier Inc., 2019, https://doi.org/10.1016/B978-0-12-815481-6.00018-X.

[22] Q. Zheng, B. Han, X. Cui, X. Yu, J. Ou, Graphene-engineered cementitious composites: small makes a big impact, 7 (2017) 1–18. https://doi.org/10.1177/1847980417742304.

[23] K.J.D. Mackenzie, Æ.M.J. Bolton, Electrical and mechanical properties of aluminosilicate inorganic polymer composites with carbon nanotubes, (2009) 2851–2857. https://doi.org/10.1007/s10853-009-3377-z.

[24] H.M. Khater, H.A.A. Gawaad, Characterization of alkali activated geopolymer mortar doped with MWCNT, 102 (2016) 329–337. https://doi.org/10.1016/j.conbuildmat.2015.10.121.

[25] M. Saafi, K. Andrew, P. Leung, D. Mcghon, S. Taylor, M. Rahman, S. Yang, X. Zhou, Multifunctional properties of carbon nanotube / fly ash geopolymeric nanocomposites, Constr. Build. Mater. 49 (2013) 46–55, https://doi.org/10.1016/j.conbuildmat.2013.08.007.

[26] M. Saa, L. Tang, J. Fung, M. Rahman, Graphene / fl y ash geopolymeric composites as self-sensing structural materials, (2014). https://doi.org/10.1088/0964-1726/23/6/065006.

[27] N. Ranjbar, M. Mehrali, M. Mehrali, U.J. Alengaram, M. Zamin, Cement and Concrete Research Graphene nanoplatelet- fly ash based geopolymer composites, Cem. Concr. Res. 76 (2015) 222–231, https://doi.org/10.1016/j.cemconres.2015.06.003.

[28] Q. Liu, Q. Xu, Q. Yu, R. Gao, T. Tong, Experimental investigation on mechanical and piezoresistive properties of cementitious materials containing graphene and graphene oxide nanoplatelets, Constr. Build. Mater. 127 (2016) 565–576, https://doi.org/10.1016/j.conbuildmat.2016.10.024.

[29] D. Dimov, I. Amit, O. Gorrie, M.D. Barnes, N.J. Townsend, A.I.S. Neves, F. Withers, S. Russo, M.F. Craciun, Ultrahigh performance nanoengineered graphene – concrete composites for multifunctional applications, 1705183 (2018). https://doi.org/10.1002/adfm.201705183.

[30] I. Papanikolaou, N. Arena, A. Al-tabbaa, Graphene nanoplatelet reinforced concrete for self-sensing structures e a lifecycle assessment perspective, J. Clean. Prod. 240 (2019) 118202, https://doi.org/10.1016/j.jclepro.2019.118202.

[31] M. Chougan, E. Marotta, F.R. Lamastra, F. Vivio, G. Montesperelli, U. Ianniruberto, A. Bianco, A systematic study on EN-998-2 premixed mortars modified with graphene-based materials, Constr. Build. Mater. 227 (2019) 116701, https://doi.org/10.1016/j.conbuildmat.2019.116701.

[32] S. Yaseri, G. Hajiaghaei, F. Mohammadi, M. Mahdikhani, R. Farokhzad, The role of synthesis parameters on the workability, setting and strength properties of binary binder based geopolymer paste, Constr. Build. Mater. 157 (2017) 534–545, https://doi.org/10.1016/j.conbuildmat.2017.09.102.

[33] A. Milev, M. Wilson, G.S.K. Kannangara, N. Tran, X-ray diffraction line profile analysis of nanocrystalline graphite, 111 (2008) 346–350. https://doi.org/10.1016/j.matchemphys.2008.04.024.

[34] S. Yan, P. He, D. Jia, Z. Yang, X. Duan, S. Wang, In situ fabrication and characterization of graphene / geopolymer composites, Ceram. Int. 41 (2015) 11242–11250, https://doi.org/10.1016/j.ceramint.2015.05.075.

[35] N. Ranjbar, M. Mehrali, U.J. Alengaram, H. Simon, C. Metselaar, Compressive strength and microstructural analysis of fly ash / palm oil fuel ash based geopolymer mortar under elevated temperatures, Constr. Build. Mater. 65 (2014) 114–121, https://doi.org/10.1016/j.conbuildmat.2014.04.064.

[36] T.T. Le, S.A. Austin, S. Lim, R.A. Buswell, A.G.F. Gibb, T. Thorpe, Mix design and fresh properties for high-performance printing concrete, (2012) 1221–1232. https://doi.org/10.1617/s11527-012-9828-z.

[37] F. Bos, R. Wolfs, Z. Ahmed, T. Salet, Additive manufacturing of concrete in construction: potentials and challenges of 3D concrete printing, 2759 (2016). https://doi.org/10.1080/17452759.2016.1209867.

[38] G. Ma, Z. Li, L. Wang, Printable properties of cementitious material containing copper tailings for extrusion based 3D printing, Constr. Build. Mater. 162 (2018) 613–627, https://doi.org/10.1016/j.conbuildmat.2017.12.051.

[39] A. Kazemian, X. Yuan, E. Cochran, B. Khoshnevis, Cementitious materials for construction-scale 3D printing: laboratory testing of fresh printing mixture, Constr. Build. Mater. 145 (2017) 639–647, https://doi.org/10.1016/j.conbuildmat.2017.04.015.

[40] V. Ungheria, Rheological models for cement pastes, 325 (1988) 41–46.

[41] S. Kashif, U. Rehman, Z. Ibrahim, M. Jameel, S.A. Memon, M.F. Javed, M. Aslam, K. Mehmood, S. Nazar, Assessment of rheological and piezoresistive properties of graphene based cement composites, Int. J. Concr. Struct. Mater. (2018), https://doi.org/10.1186/s40069-018-0293-0.

[42] W. Long, H. Li, C. Fang, F. Xing, Uniformly Dispersed and Re-Agglomerated Graphene Oxide-Based Cement Pastes: A Comparison of Rheologic Properties, Mechanical Properties and Mic, (2018). https://doi.org/10.3390/nano8010031.

[43] F. Celik, H. Canakci, An investigation of rheological properties of cement-based grout mixed with rice husk ash (RHA), Constr. Build. Mater. 91 (2015) 187–194, https://doi.org/10.1016/j.conbuildmat.2015.05.025.

[44] M. Chen, L. Li, Y. Zheng, P. Zhao, L. Lu, X. Cheng, Rheological and mechanical properties of admixtures modified 3D printing sulphoaluminate cementitious materials Rheological and mechanical properties of admixtures modified 3D printing sulphoaluminate cementitious materials, (2018). https://doi.org/10.1016/j.conbuildmat.2018.09.037

[45] Y. Rifaai, A. Yahia, A. Mostafa, S. Aggoun, E. Kadri, Rheology of fly ash-based geoolymer: effect of NaOH concentration, Constr. Build. Mater. 223 (2019) 583–594, https://doi.org/10.1016/j.conbuildmat.2019.07.028.

[46] G. Ishwarya, B. Singh, S. Deshwal, S.K. Bhattacharyya, Effect of sodium carbonate / sodium silicate activator on the rheology, geopolymerization and strength of fly ash / slag geopolymer pastes, Cem. Concr. Compos. 97 (2019) 226–238, https://doi.org/10.1016/j.cemconcomp.2018.12.007.

[47] G. Luz, P. Jean, P. Gleize, E.R. Batiston, F. Pelisser, Effect of pristine and functionalized carbon nanotubes on microstructural, rheological, and mechanical behaviors of metakaolin-based geopolymer, Cem. Concr. Compos. 104 (2019), https://doi.org/10.1016/j.cemconcomp.2019.05.015 103332.

[48] M. Romagnoli, C. Leonelli, E. Kamse, M.L. Gualtieri, Rheology of geopolymer by DOE approach, Constr. Build. Mater. 36 (2012) 251–258, https://doi.org/10.1016/j.conbuildmat.2012.04.122.

[49] A. Bhowmick, S. Ghosh, Effect of synthesizing parameters on workability and compressive strength of Fly ash based Geopolymer mortar, 3 (2012) 168–177. https://doi.org/10.6088/ijcser.201203013016.

[50] H. Alghamdi, S.A.O. Nair, N. Neithalath, Insights into material design, extrusion rheology, and properties of 3D- printable alkali-activated fl y ash-based binders, Mater. Des. 167 (2019) 107634, https://doi.org/10.1016/j.matdes.2019.107634.

[51] A. Lampropoulos, A. Cundy, Effect of alkaline activator, water, superplasticiser and slag contents on the compressive strength and workability of slag-fly ash based geopolymer mortar cured under, Ambient Temp. (2016).

[52] J. Xiang, L. Liu, X. Cui, Y. He, G. Zheng, C. Shi, Effect of fuller- fine sand on rheological, drying shrinkage, and microstructural properties of metakaolin-based geopolymer grouting materials, Cem. Concr. Compos. 104 (2019) 103381, https://doi.org/10.1016/j.cemconcomp.2019.103381.

[53] A. De Rossi, M.J. Ribeiro, J.A. Labrincha, R.M. Novais, D. Hotza, R.F.P.M. Moreira, Effect of the particle size range of construction and demolition waste on the fresh and hardened-state properties of fly ash-based geopolymer mortars with total replacement of sand, Process Saf. Environ. Prot. 129 (2019) 130–137, https://doi.org/10.1016/j.psep.2019.06.026.

[54] P. Nath, P. Kumar, V.B. Rangan, Early age properties of low-calcium fly ash geopolymer concrete suitable for ambient curing, Procedia Eng. 125 (2015) 601–607, https://doi.org/10.1016/j.proeng.2015.11.077.

[55] H.E. Elyamany, A. Elmoaty, M.A. Elmoaty, A.M. Elshaboury, Setting time and 7-day strength of geopolymer mortar with various binders, Constr. Build. Mater. 187 (2018) 974–983, https://doi.org/10.1016/j.conbuildmat.2018.08.025.

[56] G.M. Rao, T.D.G. Rao, Final setting time and compressive strength of fly ash and GGBS-based geopolymer paste and mortar, (2015) 3067–3074. https://doi.org/10.1007/s13369-015-1757-z.

[57] R. Lediga, D. Kruger, Optimizing concrete mix design for application in 3d printing technology for the construction industry, 263 (2017) 24–29. https://doi.org/10.4028/www.scientific.net/SSP.263.24.

[58] B. Panda, C. Unluer, M. Jen, Extrusion and rheology characterization of geopolymer nanocomposites used in 3D printing, Compos. Part B. 176 (2019) 107290, https://doi.org/10.1016/j.compositesb.2019.107290.

[59] J. Xie, J. Wang, R. Rao, C. Wang, C. Fang, Effects of combined usage of GGBS and fly ash on workability and mechanical properties of alkali activated geopolymer concrete with recycled aggregate, Compos. Part B 164 (2019) 179–190, https://doi.org/10.1016/j.compositesb.2018.11.067.

[60] J.G. Sanjayan, B. Nematollahi, M. Xia, T. Marchment, Effect of surface moisture on inter-layer strength of 3D printed concrete, Constr. Build. Mater. 172 (2018) 468–475, https://doi.org/10.1016/j.conbuildmat.2018.03.232.

[61] A. Peled, S.P. Shah, Processing effects in cementitious composites: extrusion and casting, (2003) 192–199.

[62] B. Panda, S.C. Paul, L.J. Hui, Y.W.D. Tay, M.J. Tan, Additive manufacturing of geopolymer for sustainable built environment, J. Clean. Prod. 167 (2018) 281–288, https://doi.org/10.1016/j.jclepro.2017.08.165.

[63] H. Yang, H. Cui, W. Tang, Z. Li, N. Han, F. Xing, A critical review on research progress of graphene / cement based composites, Compos. Part A 102 (2017) 273–296, https://doi.org/10.1016/j.compositesa.2017.07.019.

[64] W. Meng, K.H. Khayat, Effect of graphite nanoplatelets and carbon nanofibers on rheology, hydration, shrinkage, mechanical properties, and microstructure of UHPC, Cem. Concr. Res. (2018), https://doi.org/10.1016/j.cemconres.2018.01.001.